

# Water-soluble derivatives of chitosan as a target delivery system of $^{99m}\text{Tc}$ to some organs in vivo for nuclear imaging and biodistribution

Dalia L. Hawary · Mohamed A. Motaleb ·  
Hamed Farag · Osiris W. Guirguis ·  
Maher Z. Elsabee

Received: 9 June 2011 / Published online: 5 July 2011  
© Akadémiai Kiadó, Budapest, Hungary 2011

**Abstract** Carboxymethyl chitosan, (CMC), and *N*-lauryl-carboxymethyl chitosan (LCMC), have been prepared as water soluble derivatives of chitosan. These biodegradable chitosan derivatives were characterized and investigated for nuclear imaging and body distribution. They were labeled with  $^{99m}\text{Tc}$  to use them as targeted delivery to some organs in vivo for nuclear imaging and to follow their biodistribution within the body. The factors controlling the labeling efficiency have been investigated. The percent labeling yield was determined by using ascending paper chromatographic technique. In vivo biodistribution studies of radiolabeled chitosan derivatives were carried out in groups of female Wistar rats, the body distribution profile in rat was recorded by gamma scintigraphy and the biodistribution of  $^{99m}\text{Tc}$ -labeled compounds in each organ was calculated as a percentage of the injected dose per gram of tissue (%ID/g). It has been found that the biodistribution of the two compounds and the pattern of their liver uptake were markedly different. The present study demonstrates a high potential approach for liver imaging using  $^{99m}\text{Tc}$ -

LCMC. An intriguing finding of this study was that the three samples were excreted rapidly via the kidneys because of the water-soluble nature of chitosan derivatives. This suggests that water-soluble chitosan derivatives are good polymeric carriers for radioactive element that overcomes accumulation in the body. Moreover, the easy and inexpensive availability of chitosan could be beneficial for applications in scintigraphic imaging.

**Keywords**  $^{99m}\text{Tc}$  · Gamma scintigraphy · Targeted delivery · Carboxy methyl chitosan · *N*-Lauryl-carboxymethyl chitosan · Biodistribution

## Introduction

Polymeric materials provide the most important avenues for research concerning drug delivery systems, primarily because of their ease of processing and the ability to control their chemical and physical properties. Increasing attention has been given to designing polymeric drug carriers that are biodegradable, non-toxic, tissue and body-compatible. Chitosan is one of the most favorable candidates, which possesses these characteristics [1].

Chitosan is obtained from chitin by heterogeneous alkaline deacetylation using concentrated NaOH solutions. Among numerous possible applications, chitosan seems to be a very promising candidate for the development of drug delivery systems [2, 3]. The solubility, conformation, and dimensions of chitosan chains in aqueous media have been extensively studied as a function of the degree of acetylation (DA) [4]. However the application of chitosan was limited owing to the insolubility at neutral or high pH region. To improve the soluble property of chitosan, generally, chemical modification is required.

---

D. L. Hawary · O. W. Guirguis  
Department of Biophysics, Faculty of Science, Cairo University,  
Cairo 12613, Egypt

M. A. Motaleb  
Department of Labeled Compounds, Hot Labs Center, Atomic  
Energy Authority, Cairo, Egypt

H. Farag  
Departement of Nuclear Engineering, Faculty of Engineering,  
King-Abdoulziz, Jeddah, Saudi Arabia

M. Z. Elsabee (✉)  
Department of Chemistry, Faculty of Science, Cairo University,  
Cairo 12613, Egypt  
e-mail: mzelsabee@yahoo.com

It was reported [5] that the *N*-acyl and *N*-alkyl derivatives of chitosan having carboxy or sulfate group are soluble at basic pH region. Moreover, some of chitosan derivatives substituted with saccharides are soluble at all pH ranges and were stable for at least 2 weeks. These derivatives would be useful for the treatment at neutral or basic pH region to test biological activities *in vitro* and *in vivo*.

The transport and accumulation into the target organ is an important issue for  $^{99m}\text{Tc}$  radiopharmaceuticals development. The development of radiopharmaceuticals designed to bind specific receptors, including membrane transport systems, is receiving much interest due to their potential to achieve improved *in vivo* monitoring of biochemical and physiological functions [6]. Technetium-99m ( $^{99m}\text{Tc}$ ) is the radionuclide of choice for diagnostic imaging with single photon emission computed tomography (SPECT) due to its ideal nuclear properties ( $E\gamma = 140$  keV,  $T_{1/2} = 6$  h, no  $\beta$ -emission) and availability from a  $^{99}\text{Mo}/^{99m}\text{Tc}$  generator [6].

These properties have led to the search of novel  $^{99m}\text{Tc}$ -based radiopharmaceuticals incorporating ligands specifically designed to probe protein receptors and transporters as examples: for bone imaging [7, 8], myocardial perfusion imaging [9], brain imaging [10] and urinary bladder imaging [11].

Shah and coworkers [12–14] have published a series of papers dealing with the preparation, characterization and biological evaluation of  $^{99m}\text{Tc}$  complexes. These complex were prepared for the *in vivo* scintigraphic localization of the *Staphylococcus aureus* infectious foci in male Wister rats' model.

Miwa et al. [15] reported that water soluble polymers with negative charges are taken up by the liver via scavenger receptor mediated mechanism and that LCMC is effective as passive targeting carrier to liver.

Chitosan derivatives were also thought to chelate with  $^{99m}\text{Tc}$  [16] because of the amine group of *D*-glucosamine which allows them to be used as nuclear imaging radiopharmaceuticals for targeting hepatocytes. Recently, there have been many studies of liver-targeting systems using methods such as passive trapping of microparticles by reticuloendothelium [17] or active targeting based on hepatic-receptor recognition [18, 19]. Active targeting utilizing receptor recognition can be attained using molecules with receptor specific ligands. The biochemical characteristics of the hepatic asialoglycoprotein receptor, localized on the liver parenchymal cells, have been investigated in detail [20], and this receptor has been utilized as a useful site for liver targeting by many researchers [21, 22]. Since the galactose moiety is recognized specifically by the asialoglycoprotein receptor, also some polymers and other materials containing ligands such as lactose

[23] have been studied to target hepatocytes for delivery of drugs or genes. More over some radiolabeled proteins have been synthesized with galactose or lactose residue for targeting hepatocytes [24].

In this study, two different water soluble derivatives of chitosan; Carboxymethylation chitosan (CMC) and *N*-lauryl-carboxymethyl chitosan (LCMC) were prepared to be used as a targeted delivery of  $^{99m}\text{Tc}$  to some organs *in vivo* for nuclear imaging and bio-distribution studies.

CMC among the water-soluble chitosan derivatives is an amphiprotic ether derivative that contains  $-\text{COOH}$  groups and  $-\text{NH}_2$  groups in the molecule. The structure, antibacterial activity, toxicity and membrane properties of *N*- and *O*-carboxymethyl-chitosan have been previously reported [25, 26].

*O*-Carboxymethyl chitosan (OCMC) is a very promising candidate for applications demanding cell and blood compatibility [27, 28].

LCMC has the lauryl groups attached to the amino groups provide the hydrophobic moieties and, the carboxymethyl groups attached to hydroxy groups provide the hydrophilic moieties. This polymer can be used as a drug carrier to some poorly soluble anticancer drugs as Taxol, by the micelles forming mechanism [15]. It also has the advantage of being water soluble and can be therefore suitable to be labeled with radioactive cations (for example technetium-99m,  $^{99m}\text{Tc}$ ) for imaging purposes specifically in the *in vivo* studies.

Labeling efficiency and stability study for these compounds with  $^{99m}\text{Tc}$  are performed using ascending paper chromatographic technique [29, 30] considering time of the reaction, the effect of substrate amount, the effect of  $\text{SnCl}_2$  concentration, and the effect of pH of the reaction mixture in order to approach the optimum conditions for labeling.

Investigation for nuclear imaging and body distribution are performed in female Wistar rats as an animal model. The body distribution profile of rats is recorded by gamma scintigraphy and the biodistribution of  $^{99m}\text{Tc}$ -labeled compounds in each organ was calculated as a percentage of the injected dose per gram of tissue (%ID/g).

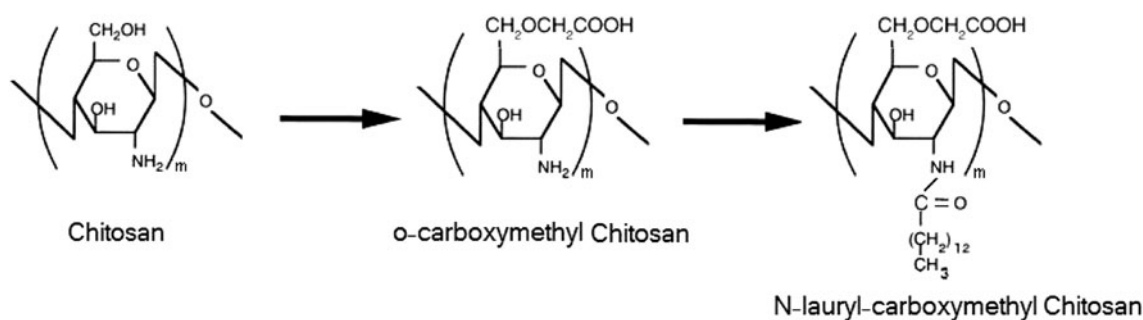
## Materials and methods

### Preparation methods

#### *Preparation of chitosan*

Chitin is extracted from shrimp shells, according to Ref. [31].

The extraction process involves three steps, removal of calcium carbonate, protein and other pigments from the shells leaving a chitin only.



**Scheme 1** Preparation of *O*-carboxymethyl chitosan and *N*-lauryl-carboxymethyl chitosan

The deacetylation of chitin involves alkali treatment (40% sodium hydroxide at 120 °C for 1–3 h, the alkali removes the protein and deacetylates the chitin simultaneously. Depending on the used alkali concentration, some soluble glycans are removed, this treatment produces 70% deacetylated chitosan. To obtain higher percent of deacetylation, this process should be repeated several times [32].

Purification of chitosan is done by dissolving the chitosan in 2% w/v acetic acid. Then the insoluble material is removed giving a clear supernatant solution, which is neutralized with NaOH solution resulting in a purified sample of chitosan.

#### Preparation of carboxymethyl chitosan

Carboxymethyl chitosan was prepared by the method of Liu et al. [25] with slight modification. Chitosan (1 g), sodium hydroxide (3 g), and solvent (4 mL H<sub>2</sub>O + 8 mL isopropanol) were added into a flask (500 mL) to swell and alkalize at a –14 °C temperature overnight.

Monochloroacetic acid (4 g) was dissolved in isopropanol (8 mL), and added into the reaction mixture drop wise for 30 min. The temperature was maintained in a water bath at 50 °C and reacted for 12 h at the same temperature, then stopped by adding 70% ethyl alcohol (200 mL).

The solid was filtered and rinsed in 70–90% ethyl alcohol to desalt and dewater. The product is the Na salt, which was dissolved in water and precipitated with ethyl alcohol.

#### Preparation of *N*-lauryl-carboxymethyl chitosan

After preparing CMC by the method mentioned above, 1 g of CMC was dissolved in 10 mL of water with mechanical stirring then 10 mL of methanol was added. Lauryl chloride equivalent per amino group of chitosan was added (1.43 mL) and the reaction mixture was stirred at room

temperature overnight. LCMC was precipitated with methanol.

Preparation process of *O*-carboxymethyl chitosan and *N*-lauryl-carboxymethyl chitosan is represented in Scheme 1.

#### Characterization of chitosan and chitosan derivatives

##### Determination of the degree of deacetylation of chitosan

The elemental composition of all samples was determined using Perkin-Elmer PE 2400 CHN, elemental analyzer, in the Micro Analytical Unit in Cairo University. Potentiometric titration was used for the determination of the degree of deacetylation of chitosan. FTIR spectroscopy was measured using Perkin-Elmer 2000 spectrophotometer [33].

Viscosity measurements of the extracted chitosan and its derivatives were determined using Ubbelohde viscometer. The flow times of the solution and solvent were recorded in second and are used to calculate the intrinsic viscosity,  $[\eta]$  which is taken as a measure of the molecular weight. The intrinsic viscosity of chitosan was measured using 2% acetic acid containing 0.2 M sodium chloride solution. The intrinsic viscosity of NSC and LNSC was measured using 0.1 M aqueous NaCl as a solvent.

**Labeling efficiency and stability study** The percent labeling yield was determined by using ascending paper chromatographic technique, the mobility of reduced forms of  $^{99m}\text{Tc}$  and free pertechnetate anion was observed. Hydrolyzed form of  $^{99m}\text{Tc}$  remains at the starting position ( $R_f = 0$ ) while free pertechnetate anion ( $^{99m}\text{TcO}_4^-$ ) moves with the solvent front ( $R_f = 1$ ) when ITLC is used as separation method [10, 11, 34].

A paper strips of silica gel impregnated glass fiber sheets (ITLC-SG) (Gelman Sciences Inc., Ann Arbor, MI, USA), 10 × 1.5 cm, were marked gently with a pencil at a distance of 2 cm from the lower end. A spot from the reaction

mixture was applied at this line, and then the strip was developed in an ascending manner in a closed jar filled with  $N_2$  gas to prevent oxidation of the labeled complex. The developing solvents; acetone and ethanol: water: ammonium hydroxide mixture (2:5:1) purged with  $N_2$  gas for the same purpose. After complete development, the strips were dried and count in a well-type gamma-scintillation counter. The organic solvent acetone was used to calculate the percent of free  $^{99m}TcO_4^-$  which moved with the solvent front ( $R_f = 1$ ) leaving the labeled complex and colloid at the origin. Ethanol:water:ammonium hydroxide mixture (2:5:1) was used to check the amount of reduced hydrolyzed technetium which remains at the origin ( $R_f = 0$ ) while other species migrate with the solvent front ( $R_f = 1$ ). The radiochemical purity was determined by subtracting the sum of the % of colloid and free pertechnetate from 100%.

This experiment was conducted to study the different factors that affect labeling yield such as: (1) tin content, (2) substrate content, (3) pH of the reaction and (4) reaction time.

In the process of labeling, trials and errors were performed for each factor under investigations till the optimum value is attained.

*Radio-labeling of chitosan derivatives with  $^{99m}Tc$*  According to the data collected from the labeling yield studied in the previous section, the best condition for preparing the radiolabeled samples of chitosan derivatives injected in vivo could be determined.

*Radio-labeling of carboxymethyl chitosan with  $^{99m}Tc$*  Accurately weighed 3.0 mg CMC was transferred to an evacuated penicillin vial. Exactly 100.0  $\mu g$   $SnCl_2$  solution was added and the pH of the mixture was adjusted to 8 using phosphate buffer, then the volume of the mixture was adjusted to 2 mL by  $N_2$ -purged phosphate buffer. One mL of freshly eluted  $^{99m}TcO_4^-$  (1.2 mCi) was added to the above mixture. The reaction mixture was vigorously shaken and allowed to react at room temperature for 10 min to complete the reaction.

*Radio-labeling of N-lauryl-carboxymethyl chitosan with  $^{99m}Tc$*  Accurately weighed 2.5 mg N-lauryl-carboxymethyl chitosan was transferred to an evacuated penicillin vial. Exactly 50.0  $\mu g$   $SnCl_2$  solution was added and the pH of the mixture was adjusted to 5 using phosphate buffer, then the volume of the mixture was completed to 1 mL by  $N_2$ -purged phosphate buffer. One mL of freshly eluted  $^{99m}TcO_4^-$  (1.2 mCi) was added to the above mixture. The reaction mixture was vigorously shaken and allowed to react at room temperature for sufficient time required to complete the reaction.

## Gamma scintigraphy

Dual-Head Variable Angle Gamma Camera From Siemens, in the Nuclear Medicine Unit of the National Cancer Institute, Cairo University, Egypt, was used in the present work.

The body distribution profile in rat was recorded in the gamma camera with a 5-mm pinhole collimator, window setting of 140 keV, and 20% width.

For gamma-imaging studies, female Wistar rats weighting between 120.0 and 150.0 g were purchased from the animal house at the National Cancer Institute, Cairo University. After intravenous administration of radiolabeled CMC and LCMC (injected dose: 0.5 mg CMC in 0.5 mL phosphate buffer, activity: 0.2 mCi) and (injected dose: 0.625 mg LCMC in 0.5 mL phosphate buffer, activity: 0.3 mCi), respectively, the animal was anesthetized by intramuscular injection of xylazine (10.0 mg/kg) and 0.5 mL ketamine hydrochloride (100.0 mg/kg) few minutes before imaging. Those doses were given according to Laboratory Animal Sciences Program in NCI Fredric Center for Cancer Research and this anesthetic agent is believed to have a negligible effect on both blood pressure and the biodistribution of the radiolabeled samples.

The Dose Rate Calibrator was used for measuring the radioactive dose administered to the rat, the dose rate Calibrator is a Well Ion Chamber Detector, manufactured by Capintec Company, USA.

Then the animal was fixed promptly on a board in posterior anterior position and imaging was performed at different time intervals using a gamma camera. The images were taken in the two positions anterior and posterior.

Gamma camera images were acquired at 20, 60, and 120 min after injection. The static images were stored in a  $512 \times 512$  matrix size and acquisition times were 300 s [35].

## Biodistribution of radiolabeled derivatives of chitosan

In vivo biodistribution studies were carried out in groups of twelve female Wistar rats, where each animal was injected in the tail vein with the earlier determined doses of  $^{99m}Tc$  labeled chitosan derivatives. The lateral tail vein was successfully located after a little practice with a canola of size 24. The rats were put in metabolic cages for the required time. The rats were sacrificed by slitting their throats in 3 groups of four rats at various time intervals (20, 60, and 120 min) after injection and the organs of interest (liver, kidney, muscle, blood, intestine, bone, spleen, stomach and heart) were removed. Dissected tissue samples rinsed of excess blood, weighted and counted in a gamma counter.

To correct for physical decay and to calculate uptake of the radiolabel in each tissue sample as a fraction of the injected dose, aliquots of the injected dose were counted simultaneously. The biodistribution results were expressed as percentage injected dose per gram of tissue or organ (% ID/g), the total counts injected per animal were calculated by the difference between the original syringe counts and the remaining syringe counts after injection.

## Results and discussion

### Synthesis and characterizations

Determination of the degree of deacetylation (DDA) and characterization for chitosan, CMC, and LCMC are outlined by elemental analysis, potentiometric titration and FTIR spectra.

Determination of the molecular weight of chitosan was done by determining the intrinsic viscosity.

### Elemental analysis

The elemental composition of chitosan samples was determined as follows: found (calculated) %: C = 40.71 (44.7), H = 6.12 (6.8), N = 7.50 (8.6).

The DDA% value of chitosan was calculated from the following formula [36]:

$$\text{DDA}\% = \frac{6.857 - \text{C/N}}{1.7143} \times 100 = 88.33$$

The elemental analysis of CMC and LCMC were as follow: CMC Found (calculated): C = 35.8 (43.8), H = 5.21 (5.9), N = 4.88 (6.4) and for LCMC Found (calculated): C = 53.43 (60.2), H = 6.4 (8.7), N = 3.26 (3.55).

The percentage of carbon (C%), nitrogen (N%) and hydrogen (H%) in CMC and LCMC, by comparing the C/N molar ratio the degree of substitution were calculated. The increase in the molar ratio indicates the increasing carbon in chitosan chain, since the monosaccharide include one nitrogen atom.

The degree of carboxymethylation was estimated from the increasing-molar ratio/2 since the carboxymethyl group includes 2 carbons and was found to be 1.0.

The degree of substitution DS of LCMC was estimated in the same way and was found to be 0.53.

**Potentiometric titration** Potentiometric titration was used to determine the DDA% of the prepared chitosan.

The degree of acetylation (DA%) of the chitosan was calculated using the following formula [37]:

$$\text{DA}\% = \frac{1 - 161Q}{1 + 42Q} \times 100$$

where  $Q = N \times \Delta V/m$ ,  $\Delta V$  is the volume of NaOH between the two inflection points (in L),  $N$  is the normality of the sodium hydroxide and  $m$  is the weight of the dry chitosan (in g). From the calculation it was found that DDA% of chitosan = 87.3%.

**FTIR spectroscopy** Figure 1 shows the FTIR spectra of chitosan, CMC and LCMC.

It was found from the spectrum of chitosan that distinctive absorption bands appear at  $1653\text{ cm}^{-1}$  (Amide I),  $1597\text{ cm}^{-1}$  ( $-\text{NH}_2$  bending) and  $1375\text{ cm}^{-1}$  (Amide III). The absorption bands at  $1151\text{ cm}^{-1}$  (asymmetric stretching of the C–O–C bridge),  $1074\text{ cm}^{-1}$  (skeletal vibration involving the C–O stretching), at  $3384\text{ cm}^{-1}$  (O–H stretch),  $2880\text{ cm}^{-1}$  (C–H stretch) and  $1320\text{ cm}^{-1}$  (C–N stretch).

The DDA% of the samples was calculated from the IR-spectra following the method in Ref. [38] using the following equation:

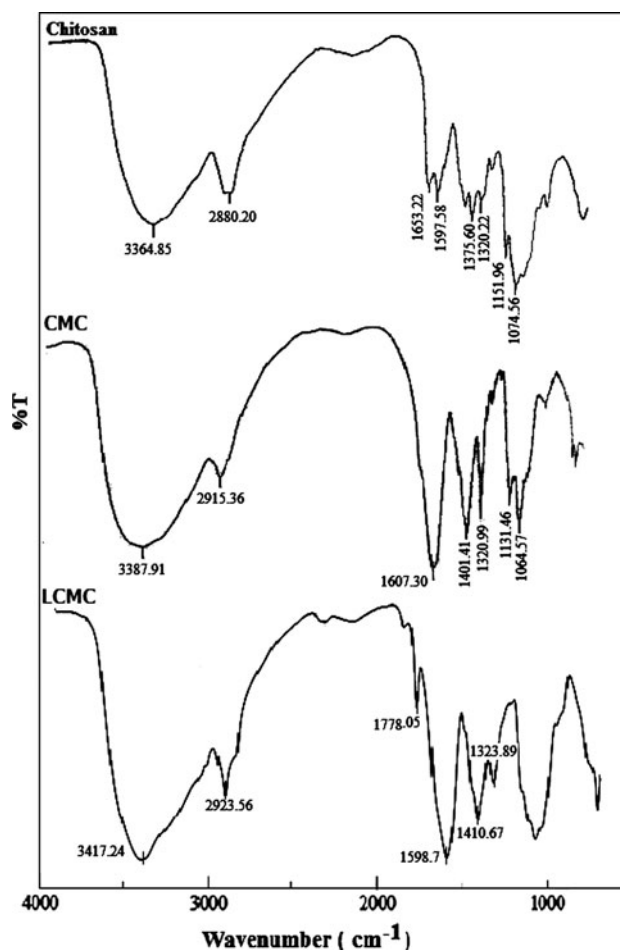


Fig. 1 FTIR spectrum of chitosan, CMC and LCMC

$$A_{1320}/A_{1420} = 0.3822 + 0.03133 \times \text{DA}$$

Therefore, by calculation,

$$\text{DA}\% = 18.44$$

and

$$\text{DDA}\% = 89.56$$

A very good agreement for DDA% between elemental analysis and potentiometric titration has been augmented by the FTIR analysis. The results were 88.33, 87.3 and 89.56 respectively.

The main characteristic bands of CMC, at 1607 and 1401  $\text{cm}^{-1}$  correspond to the asymmetrical and symmetrical stretching of  $\text{COO}^-$  group respectively. The carboxy group band at 1607  $\text{cm}^{-1}$  overlaps with N–H bend. Compared with the peaks of chitosan, the peak of CMC at 1320  $\text{cm}^{-1}$  increase, thus indicating carboxymethylation has occurred on the hydroxyl groups of chitosan.

Compared with CMC, the IR spectrum of LCMC shows a new signal at 1778  $\text{cm}^{-1}$  corresponding to carbonyl group of the lauryl. The band at 1598  $\text{cm}^{-1}$  is corresponding to ( $-\text{NH}_2$  bending) which overlaps with that of the Amide I. The increase in the band at 1598  $\text{cm}^{-1}$  indicates that the reaction takes place at carboxymethyl group at the hydroxyl group. The band at 1410  $\text{cm}^{-1}$  also increases because of the carbonyl group of the lauryl moiety.

**Intrinsic viscosity** The intrinsic viscosity was taken as indication for the molecular weight of the prepared samples it was determined by plotting  $\eta_{\text{sp}}/C$  against sample concentration.

By using: Mark–Houwink–Sakurada equation, the average molecular weight,  $M_v$ , of chitosan was calculated from  $[\eta] = 1.81 \times 10^{-3} M_v^{0.93}$  and was found to be equal to  $1.55 \times 10^4$  g/mol.

The intrinsic viscosity of the prepared CMC and LCMC decreased sharply compared to chitosan due mainly to polymer chain secession during the successive substitution reactions.  $[\eta]$  for chitosan, CMC and LCMC, was 14.25, 0.45 and 0.38 dL/g, respectively.

#### Labeling efficiency and stability study

##### *Effect of reaction time*

Figure 2 describes the effect of time upon the labeling yield of  $^{99\text{m}}\text{Tc}$ -CMC and  $^{99\text{m}}\text{Tc}$ -LCMC. In case of LCMC It was found that the best reaction conditions for  $^{99\text{m}}\text{Tc}$ -CMC were: 3 mg CMC, 100  $\mu\text{g}$   $\text{SnCl}_2$ , pH 8.

At 1-min post labeling, the yield was small and equal to 82.5% which increased gradually with time till reaching its

maximum value of 97.9% at 10 min. The yield decreases slightly with time to reach 92.5% at 420 min (7 h). In case of LCMC as shown in Fig. 3b, the best reaction conditions were: 2.5 mg LCMC, 50  $\mu\text{g}$   $\text{SnCl}_2$ , pH 3.5–5. The rate of formation of  $^{99\text{m}}\text{Tc}$ -LCMC complex was started relatively slowly where the yield was 83.8% at 1 min and the highest yield of 93.6% was achieved at 30 min then the formed complex was stable up to 420 min (7 h).

##### *Effect of substrate amount*

As shown in Fig. 3 the best reaction  $^{99\text{m}}\text{Tc}$ -CMC complex conditions were: 100  $\mu\text{g}$   $\text{SnCl}_2$ , pH 8 and 10 min reaction time.

The labeling yield of  $^{99\text{m}}\text{Tc}$ -CMC complex was increased with increasing the amount of CMC which increased from 93.5% at 0.5 mg CMC reaching the maximum value of 97.9% at 3.0 mg; after that, the formed complex decreases slightly with increasing the amount of CMC up to 7 mg to reach 96.5%. The optimum amount of carboxymethyl chitosan was 3.0 mg.

While in the case of lauryl carboxymethyl chitosan (LCMC), it was found that the best reaction conditions were: 50  $\mu\text{g}$   $\text{SnCl}_2$ , pH 3.5–5 and 30 min reaction time.

At low substrate concentration (0.5 mg), the yield for  $^{99\text{m}}\text{Tc}$ -LCMC was small and equal to 33.3%. This low labelling yields was due to the insufficient substrate concentration to form complex with all reduced technetium making the percent of colloid high (66.7%). Increasing the substrate concentration led to higher labeling yield and the maximum yield was achieved at 2.5 mg as shown in Fig. 4b. By increasing the substrate concentration over the optimum values, the labeling yield was decreased to become 88.3% at substrate concentration 4 mg.

##### *Effect of stannous chloride concentration*

While studying the pharmacokinetics and biodistribution of  $^{99\text{m}}\text{Tc}$  labeled compounds, stannous chloride ( $\text{SnCl}_2$ ) content is the most important factor affecting the labeling yield because it was found that stannous chloride and other stannous salts, when used as reducing agents, lead to the formation of colloidal tin (IV) oxide particles [39]. As a result, the biodistribution of radio-labeled chitosan derivatives might be governed by the biodistribution of tin oxide colloids alone. So it is very important to reduce the tin oxide colloids as least as possible by studying the effect of  $\text{SnCl}_2$  concentration on the labeling yield.

As shown in Fig. 4a, the best reaction conditions for  $^{99\text{m}}\text{Tc}$ -CMC were 3 mg CMC, pH 8 and 10 min reaction time.  $^{99\text{m}}\text{Tc}$ -CMC complex at low Sn(II) content, 10  $\mu\text{g}$ , the

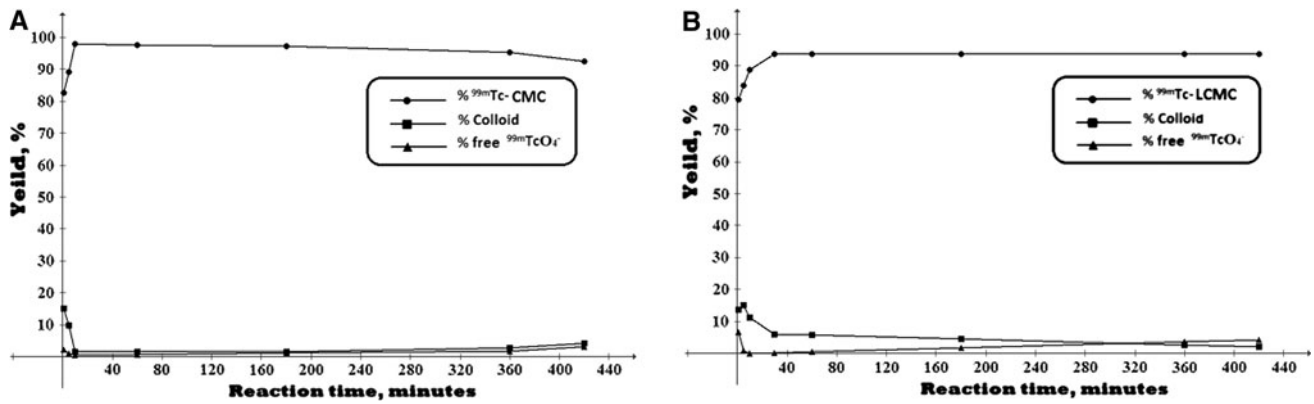


**Fig. 2** Effect of reaction time on the labeling yields of  $^{99m}\text{Tc-CMC}$  and  $^{99m}\text{Tc-LCMC}$ . **a** Reaction conditions: 3 mg CMC, 100  $\mu\text{g}$   $\text{SnCl}_2$ , pH 8. **b** Reaction conditions: 2.5 mg LCMC, 50  $\mu\text{g}$   $\text{SnCl}_2$ , pH 3.5–5

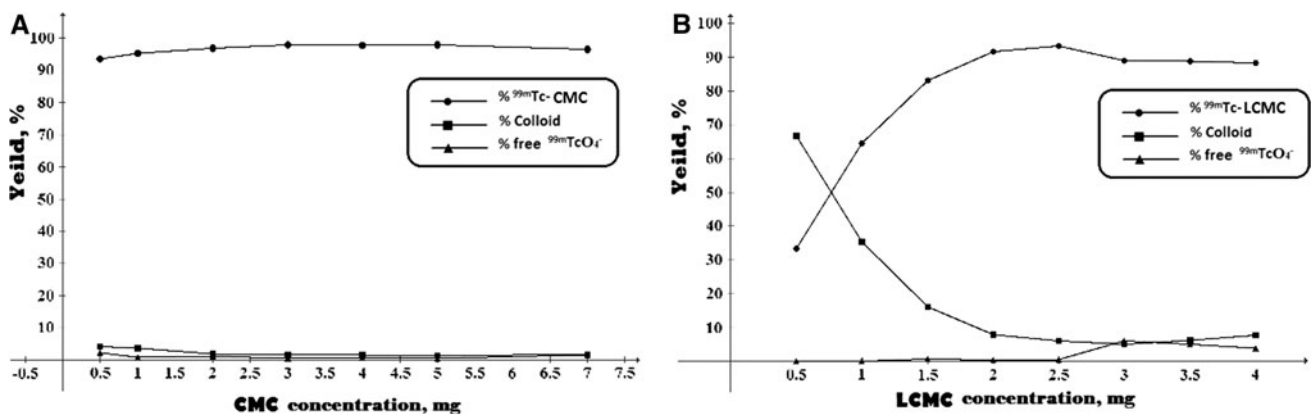


**Fig. 3** Effect of substrate amount on the labeling yield of  $^{99m}\text{Tc-CMC}$  and  $^{99m}\text{Tc-LCMC}$ . **a** Reaction conditions: 100  $\mu\text{g}$   $\text{SnCl}_2$ , pH 8 and 10 min reaction time. **b** Reaction conditions: 50  $\mu\text{g}$   $\text{SnCl}_2$ , pH 3.5–5 and 30 min reaction time

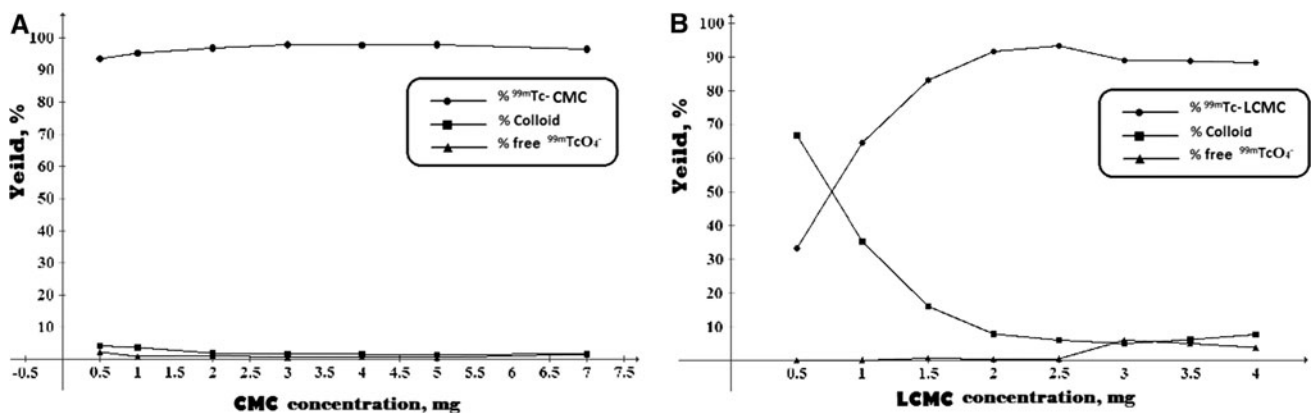


**Fig. 4** Effect of the amount of  $\text{SnCl}_2$  on the labeling yield of  $^{99m}\text{Tc-CMC}$  and  $^{99m}\text{Tc-LCMC}$ . **a** Reaction conditions: 3 mg CMC, (10–150)  $\mu\text{g}$   $\text{SnCl}_2$ , pH 8 and 10 min reaction time. **b** Reaction conditions: 2.5 mg LCMC, (30–150)  $\mu\text{g}$   $\text{SnCl}_2$ , pH 3.5–5 and 30 min reaction time

labeling yield was small and equal to 12.6% due to the amount of  $\text{Sn(II)}$  which was insufficient to reduce all  $^{99m}\text{TcO}_4^-$  (the amount of  $^{99m}\text{TcO}_4^-$  was 84.6%). By increasing the amount of  $\text{Sn(II)}$ , the labeling yield increased

till it attained the maximum value of 97.9% at 100  $\mu\text{g}$   $\text{Sn(II)}$ . When  $\text{Sn(II)}$  is increased above 100  $\mu\text{g}$ , the yield decreased again and became 55.8% at 150  $\mu\text{g}$   $\text{Sn(II)}$  due to colloid formation (41.5%).

The complexation of LCMC with technetium-99m was shown in Fig. 4b. The best reaction conditions: 2.5 mg LCMC, pH 3.5–5 and 30 min reaction time.

It shows high sensitivity to the concentration of  $\text{SnCl}_2$ , at 10  $\mu\text{g}$   $\text{SnCl}_2$ , the labeling yield of  $^{99\text{m}}\text{Tc-LCMC}$  was very small 55.2% and this low yield due to  $\text{SnCl}_2$  concentration was insufficient to reduce all pertechnetate gave a percentage of  $^{99\text{m}}\text{TcO}_4^-$  that was relatively high (25.8%). Moreover, it was observed from the figure that the yield significantly increased by increasing the amount of  $\text{SnCl}_2$  from 10 to 50  $\mu\text{g}$  (optimum content) at which maximum labeling of 93.6% was obtained. By increasing the amount of  $\text{SnCl}_2$  above 70  $\mu\text{g}$ , the yield drastically decreased to reach 18.1% at 150  $\mu\text{g}$   $\text{SnCl}_2$  that is because the excess of  $\text{SnCl}_2$  was converted to colloid.

#### Effect of pH of the reaction mixture

The effect of changing the pH of the reaction mixture was illustrated in Fig. 5. The best reaction conditions: 3 mg CMC, 100  $\mu\text{g}$   $\text{SnCl}_2$  and 10 min reaction time.

In case of  $^{99\text{m}}\text{Tc-CMC}$ , at pH 6 the labeling yield of  $^{99\text{m}}\text{Tc-CMC}$  complex was small and equal to 68.3%. This yield was increased by increasing the pH of the reaction mixture where at pH 8 the maximum labeling yield of 97.9% was attained. By increasing the pH more than 8, the labeling yield decreased and reached 87.4% at pH 9.

In case of  $^{99\text{m}}\text{Tc-LCMC}$ , Fig. 6b, the best reaction conditions: 2.5 mg LCMC, 50  $\mu\text{g}$   $\text{SnCl}_2$  and 30 min reaction time. It clearly shows that, the optimum pH required to give high labeling yield for  $^{99\text{m}}\text{Tc-LCMC}$  was in the range of pH 3.5–4.5. Above and below this pH range the yields were low (at pH 2 the yield was 70.7% and at pH 6.5 the yield was 38.4%).

#### Gamma scintigraphy imaging results

The biodistribution of  $^{99\text{m}}\text{Tc-CMC}$  and  $^{99\text{m}}\text{Tc-LCMC}$  in rats were illustrated in Fig. 6.

$^{99\text{m}}\text{Tc-CMC}$  and  $^{99\text{m}}\text{Tc-LCMC}$  were transported to the liver within a few minutes of injection, whereas the pattern of liver uptake was markedly different between the two materials. Some faint liver uptake occurred in  $^{99\text{m}}\text{Tc-CMC}$  injected rat (Fig. 6a) then it was gradually decreases with time. While the liver activity of  $^{99\text{m}}\text{Tc-LCMC}$  gradually increased until 2 h, it showed also some accumulation in the spleen (Fig. 6b). Both  $^{99\text{m}}\text{Tc-CMC}$  and  $^{99\text{m}}\text{Tc-LCMC}$  were rapidly cleared by the kidneys and released very soon by the bladder.

#### Biodistribution results

The calculations for the biodistribution of  $^{99\text{m}}\text{Tc-CMC}$  and  $^{99\text{m}}\text{Tc-LCMC}$  are summarized in Tables 1 and 2.

The values of %ID/g of some organs were illustrated at 20, 60, and 120 min after injection.

In the case of  $^{99\text{m}}\text{Tc-CMC}$  no specific targeting was shown in this experiment, but it is clear that, slight increase in distribution within the liver, blood and spleen in the first 20 min giving 7.6, 6.5 and 4.7 %ID/g, respectively, followed by decreasing in 120 min (2 h) after injection to become 3.7, 1.4 and 0.9 %ID/g, respectively.

This initial increase in the activity within the liver, blood and spleen was probably due to the blood circulation and appeared mostly within blood pool organs. This can also be noticed in gamma scintigraphy images (Fig. 6a).

In the case of  $^{99\text{m}}\text{Tc-LCMC}$  Table 2 indicates that the organs of greatest uptake were the kidneys, liver and spleen. The distribution of  $^{99\text{m}}\text{Tc-LCMC}$  within them after 20 min post injection was 27.4, 22.6 and 15.3 %ID/g,

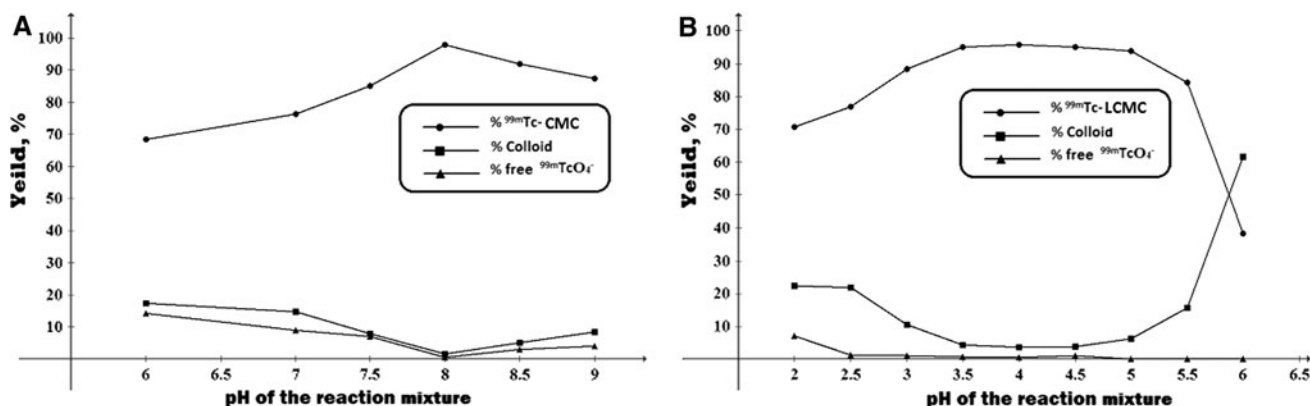


**Fig. 5** Effect of pH on the labeling yield of  $^{99\text{m}}\text{Tc-CMC}$  and  $^{99\text{m}}\text{Tc-LCMC}$ . **a** Reaction conditions: 3 mg CMC, 100  $\mu\text{g}$   $\text{SnCl}_2$ , (6–9) pH and 10 min reaction time. **b** Reaction conditions: 2.5 mg LCMC, 50  $\mu\text{g}$   $\text{SnCl}_2$ , (2–6.5) pH and 30 min reaction time



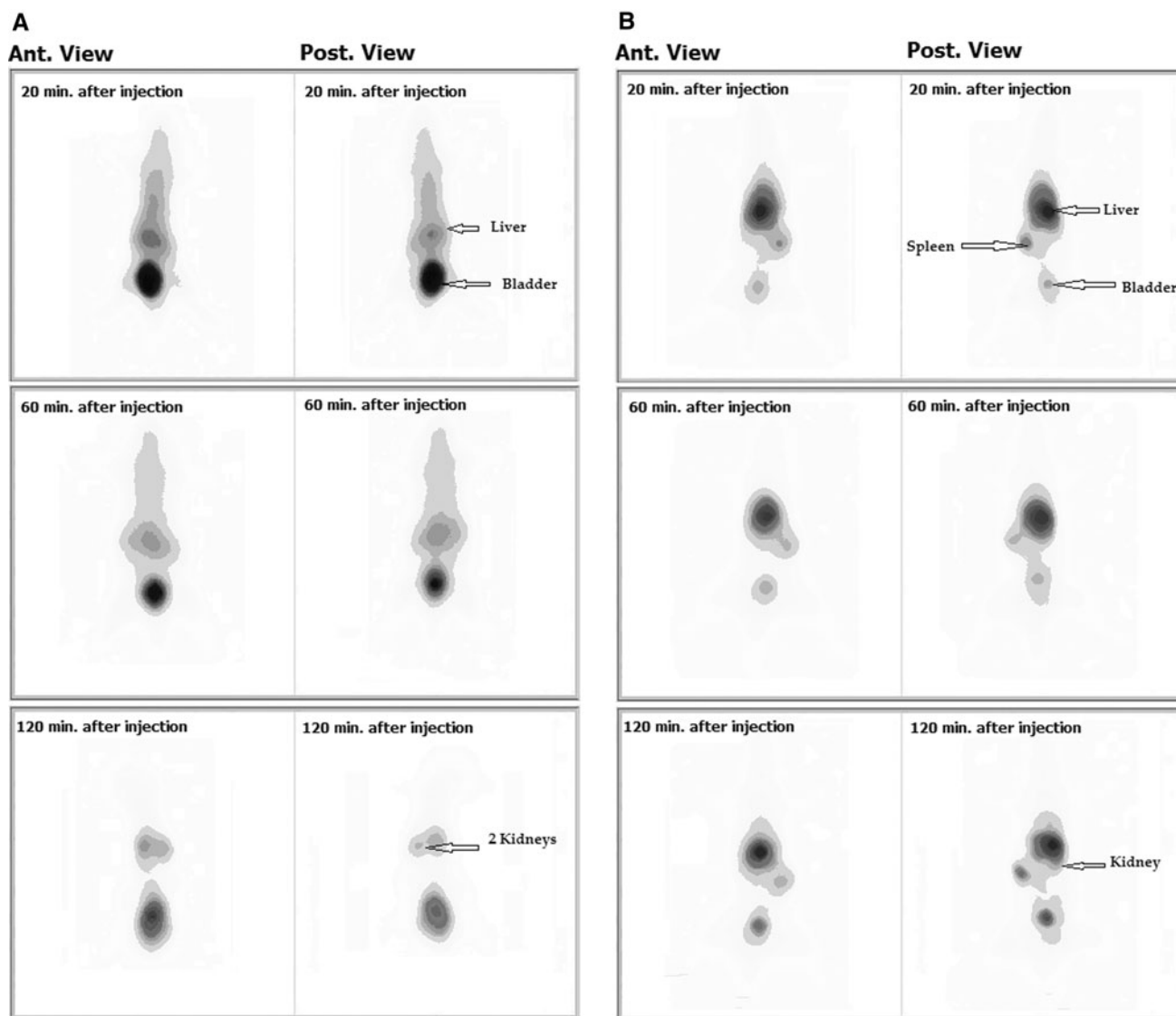


**Fig. 6** Gamma camera images of rat at 20, 60, and 120 min after injection of  $^{99m}\text{Tc}$ -CMC and  $^{99m}\text{Tc}$ -LCMC

respectively. The uptake of the liver and the spleen increase after 60 min (1 h) post injection and became 24.4 and 17.5 %ID/g, respectively, then decreased after 120 min (2 h) post injection to become 25.9 and 14.8 %ID/g.

The obtained data are in agreement with that previously obtained by Miwa et al. [15] using a similar derivative of chitosan although the functional groups in their compound are different since the product was prepared by a Schiff's base reaction with aldehydic group followed by reductive amination while in our compound it was a reaction between an acid chloride and the amino group, i.e. amide formation linkage.

Miwa also reported that LCMC has a strong negative charge which enhances phagocytosis by leucocytes for

**Table 1** The biodistribution of the  $^{99m}\text{Tc}$ -CMC in female rats

Organ	%ID/g		
	20 min $\pm$ SD (n = 4)	60 min $\pm$ SD (n = 4)	120 min $\pm$ SD (n = 4)
Liver	7.6 $\pm$ 0.7	4.1 $\pm$ 0.3	3.7 $\pm$ 0.2
Kidney	26.6 $\pm$ 1.9	21.2 $\pm$ 1.8	19.8 $\pm$ 1.6
Muscle	2.4 $\pm$ 0.1	2.5 $\pm$ 0.1	2.2 $\pm$ 0.1
Blood	6.5 $\pm$ 0.5	4.6 $\pm$ 0.3	1.4 $\pm$ 0.2
Intestine	1.5 $\pm$ 0.2	1.0 $\pm$ 0.1	0.8 $\pm$ 0.1
Bone	1.7 $\pm$ 0.1	1.5 $\pm$ 0.2	1.2 $\pm$ 0.4
Spleen	4.7 $\pm$ 0.3	2.4 $\pm$ 0.1	0.9 $\pm$ 0.1
Stomach	0.9 $\pm$ 0.1	0.8 $\pm$ 0.4	0.6 $\pm$ 0.3
Heart	1.8 $\pm$ 0.1	2.8 $\pm$ 0.1	1.1 $\pm$ 0.1

**Table 2** The biodistribution of the  $^{99m}\text{Tc}$ -LCMC in female rats

Organ	%ID/g		
	20 min $\pm$ SD ( <i>n</i> = 4)	60 min $\pm$ SD ( <i>n</i> = 4)	120 min $\pm$ SD ( <i>n</i> = 4)
Liver	22.6 $\pm$ 2.2	24.457 $\pm$ 2.2	23.705 $\pm$ 2.3
Kidney	27.4 $\pm$ 2.5	26.451 $\pm$ 2.4	25.996 $\pm$ 2.7
Muscle	1.7 $\pm$ 0.1	1.101 $\pm$ 0.1	1.063 $\pm$ 0.1
Blood	5.7 $\pm$ 0.4	4.079 $\pm$ 0.4	4.039 $\pm$ 0.4
Intestine	0.6 $\pm$ 0.1	0.802 $\pm$ 0.1	0.771 $\pm$ 0.2
Bone	1.6 $\pm$ 0.1	0.972 $\pm$ 0.2	0.673 $\pm$ 0.1
Spleen	15.3 $\pm$ 1.4	17.511 $\pm$ 1.6	14.849 $\pm$ 1.2
Stomach	1.8 $\pm$ 0.1	2.64 $\pm$ 0.1	1.769 $\pm$ 0.1
Heart	3.9 $\pm$ 0.2	3.856 $\pm$ 0.2	3.674 $\pm$ 0.2

latex size (>500 nm), it also related its uptake by liver via scavenger receptor mediated mechanism.

Based on the chemical structure of LCMC which incorporated carboxymethyl groups as hydrophilic moieties and Lauryl groups on hydrophobic moieties, Miwa considered LCMC to have hydrophobic-hydrophilic balance adequate for formation micelles that may be useful as passive targeting carriers of hydrophobic cancer drugs for solid tumors.

Data from Tables 1 and 2 also showed that  $^{99m}\text{Tc}$ -CMC and  $^{99m}\text{Tc}$ -LCMC were excreted rapidly via the kidneys and that was due to the biocompatible property of CMC [40] and the particular characteristics of the water-solubility of chitosan and its derivatives as well.

## Conclusion

In nuclear medicine three types of radiopharmaceuticals are available for liver imaging, depending on physiological function [41]. One group evaluates the potency of the biliary duct, another group evaluates the phagocytic function of the Kupffer cells; and the last group evaluates the hepatic function using a specific ligand. Targeting using specific ligands utilizes receptor recognition which can be attained using molecules with receptor specific ligands. The hepatic asialoglycoprotein receptor ASGP-R is localized on the liver parenchymal cells has been used as a useful site for liver targeting by many researchers [19]. Polymers and other materials containing ligands such as galactose [42] and lactose [23] have been studied to target hepatocytes for delivery of drugs or genes. Some radiolabeled proteins have been synthesized with galactose or lactose residue for targeting hepatocytes [24].

In the present work chitosan derivatives CMC and LCMC have been prepared. These are water soluble derivatives which are chosen as model compounds to be

used as carriers for some radioactive elements such as  $^{99m}\text{Tc}$ . This combination is found to be useful in performing hepatocyte targeted nuclear imaging. The appropriate characterizations needed to identify the chemical structure, the degree of substitution and the viscosity parameters of the prepared derivatives have been carried out.

$^{99m}\text{Tc}$  has been selected as it is one of the most useful radionuclides used in diagnostic nuclear medicine due to its outstanding properties such as its physical half-life (6.02 h) which permits the minimum effectible dose for clinical doses, its monochromatic photons (140 keV) are readily collimated to give images of superior spatial resolution. In addition, it is readily available in a sterile state from  $^{99}\text{Mo}/^{99m}\text{Tc}$  generators.

The appropriate conditions for labeling of  $^{99m}\text{Tc}$  with CMC and LCMC were investigated.

The maximum yield for labeling of 3 mg  $^{99m}\text{Tc}$ -CMC was 97.9%, when 100  $\mu\text{g}$   $\text{SnCl}_2$  was used as a reducing agent, at pH 8, at room temperature and 10 min reaction time, while the appropriate conditions for labeling of 2.5 mg  $^{99m}\text{Tc}$ -LCMC (93.6% yield) were 50  $\mu\text{g}$   $\text{SnCl}_2$  as reducing agent, at pH (3.5–5), at room temperature and 30 min reaction time.

The hepatocyte targeted nuclear imaging using  $^{99m}\text{Tc}$ -LCMC shows good targeting to the liver and it was also accumulated in the spleen, and then it began to decrease after two hours post injection.

However the liver uptake of  $^{99m}\text{Tc}$ -CMC was faint and there was rapid elimination of  $^{99m}\text{Tc}$ -CMC via the kidneys.

This study demonstrates a hopeful approach for liver imaging using  $^{99m}\text{Tc}$ - $^{99m}\text{Tc}$ -LCMC.

Even though the difficulties of controlling the molecular weight, the degree of substitution and the physical properties during the steps of synthesizes of these water soluble derivatives of chitosan, the obtained results demonstrate a hopeful approach for liver imaging using  $^{99m}\text{Tc}$ -LCMC.

An intriguing finding of the present study was that the two samples were excreted rapidly via the kidneys because of the water-soluble nature of chitosan derivatives. This suggests that water-soluble chitosan derivatives are good polymeric imaging tracers that overcome accumulation in the body.

It is noteworthy, that the easy and inexpensive availability of chitosan could be beneficial for applications in scintigraphic imaging and drug delivery researches.

## References

1. Felt O, Buri P, Gurny R (1998) Chitosan: a unique polysaccharide for drug delivery. *Drug Dev Ind Pharm* 24:979–993

2. Muzzarelli RAA (1997) Human enzymatic activities related to the therapeutical administration of chitin derivatives. *Cell Mol Life Sci* 53:131–140
3. Alishahi A, Mirvaghefi A, Tehrani MR, Farahmand H, Shojasadati A, Dorkoosh FA, Elsabee MZ (2011) Shelf life and delivery enhancement of vitamin C using chitosan nanoparticles. *J Foodchem* 126:935–940
4. Shigemasa Y, Minami S (1995) Application of chitin and chitosan for biomaterials. *Biotechnol Genet Eng Rev* 13:383–420
5. Sashiwa H, Shigemasa Y (1999) Chemical modification of chitin and chitosan 2: preparation and water soluble property of N-acylated or N-alkylated partially deacetylated chitins. *Carbohydr Polym* 39:127–138
6. Nunn AD (1992) Radiopharmaceuticals, chemistry and pharmacology. Marcel Dekker Inc, New York
7. Wang XB (2001) Synthesis and biodistribution of the  $^{99m}\text{Tc}$ -N-DMSA complex as a potential bone imaging agent. *J Radioanal Nucl Chem* 249:523–525
8. Liu L, Zhong G, Wei Y, Zhang M, Wang X (2011) Synthesis and biological evaluation of a novel  $^{99m}\text{Tc}$  complex of HYNIC-conjugated aminomethylenediphosphonate as a potential bone imaging agent. *J Radioanal Nucl Chem* 288:467–473
9. Zhang JB, Wang XB, Li CY (2002) Synthesis and biodistribution of  $^{99m}\text{Tc}$ (CHIPDTC)<sub>2</sub> as a potential myocardial perfusion imaging agent. *J Radioanal Nucl Chem* 254:99–101
10. Motaleb M, El-Kolaly M, Rashed H, Abd El-Bary A (2011) Novel radiiodinated sibutramine and fluoxetine as models for brain imaging. *J Radioanal Nucl Chem*. doi:10.1007/s10967-011-1182-z
11. Moustapha M, Motaleb M, Ibrahim I (2011) Synthesis of  $^{99m}\text{Tc}$ -oxybutynin for M3-receptor-mediated imaging of urinary bladder. *J Radioanal Nucl Chem* 287:35–40
12. Shah SQ, Khan MR (2011) Radio characterization of the  $^{99m}\text{Tc}$ -rifloxacin complex and biological evaluation in *Staphylococcus aureus* infected rat model. *J Radioanal Nucl Chem* 288:373–378
13. Shah SQ, Khan MR (2011) Radio complexation and biological characterization of the  $^{99m}\text{Tc}$ -trovafloxacin dithiocarbamate: a novel methicillin-resistant *Staphylococcus aureus* infection imaging agent. *J Radioanal Nucl Chem* 288:215–220
14. Shah SQ, Khan AU, Khan MR (2011) Radiosynthesis and biodistribution of  $^{99m}\text{Tc}$ -garenoxacin dithiocarbamate complex a potential infection imaging agent. *J Radioanal Nucl Chem* 288:59–64
15. Miwa A, Ishibe A, Nakano M, Yamahira T, Itai S, Jinno S, Kawahara H (1998) Development of novel chitosan derivatives as micellar carriers of taxol. *Pharm Res* 15:1844–1850
16. Hawary D, Motaleb M, Farag H, Guirguis O, Elsabee MZ (2011) Lactosaminated N-succinyl-chitosan as a liver targeted delivery of  $^{99m}\text{Tc}$  in vivo for nuclear imaging and biodistribution. *J Labelled Comp Radiopharm* (in press)
17. Ogawara K, Yoshida M, Higaki K, Kimura T, Shiraiishi K, Nishikawa M, Takakura Y, Hashida M (1999) Hepatic uptake of polystyrene microspheres in rats: effect of particle size on intrahepatic distribution. *J Control Release* 59:15–22
18. Fiume L, Busi C, Mattioli A (1982) Lactosaminated human serum lactosamination albumin as hepatotropic drug carrier rate of uptake by mouse liver. *FEBS Lett* 146:42–46
19. Akamatsu K, Imai M, Yamasaki Y, Nishikawa M, Takakura Y, Hashida M (1998) Disposition characteristics of glycosylated poly(amino acids) as liver cell-specific drug carrier. *J Drug Target* 6:229–239
20. Schwartz AL, Fridovich SE, Lodish HF (1982) Kinetics of internalization and recycling of the asialoglycoprotein receptor in a hepatoma cell line. *J Biol Chem* 257:4230–4237
21. Hashida M, Hirabayashi H, Nishikawa M, Takakura Y (1997) Targeted delivery of drugs and proteins to the liver via receptor-mediated endocytosis. *J Control Release* 46:129–137
22. Mahato RI, Takemura S, Akamatsu K, Nishikawa M, Takakura Y, Hashida M (1997) Physicochemical and disposition characteristics of antisense oligonucleotides complexed with glycosylated poly(L-lysine). *Biochem Pharmacol* 53:887–895
23. Choi YH, Liu F, Park JS, Kim SW (1998) Lactose-poly(ethylene glycol)-grafted poly-L-lysine as hepatoma cell-targeted gene carrier. *Bioconj Chem* 9:708–718
24. Jeong JM, Hong MK, Lee J, Son M, So Y, Lee DS, Chung JK, Lee MC (2004)  $^{99m}\text{Tc}$ -neolactosylated human serum albumin for imaging the hepatic asialoglycoprotein receptor. *Bioconj Chem* 15:850–855
25. Liu XF, Guan YL, Yang DZ, Li Z, Yao KD (2001) Antibacterial action of chitosan and carboxymethylated chitosan. *J Appl Polym Sci* 79:1324–1335
26. Zhang L, Guo J, Zhou J, Yang G, Du Y (2000) Blend membranes from carboxymethylated chitosan/alginate in aqueous solution. *Appl Poly Sci* 77:610–616
27. Cai KY, Yao KD, Li Z, Yang ZM, Li XQ (2001) Rat osteoblast functions on the O-carboxymethyl chitosan-modified poly(D,L-lactic acid) surface. *Biomater Sci* 12:1303–1315
28. Zhu AP, Zhang M, Zhang Z (2004) Surface modification of ePTFE vascular grafts with O-carboxymethylchitosan. *Polym Int* 53:15–19
29. Motaleb M (2007) Preparation of  $^{99m}\text{Tc}$ -cefoperazone complex, a novel agent. *J Radioanal Nucl Chem* 272:95–99
30. Mostafa M, Motaleb M, Sakr T (2010) Labeling of ceftriaxone for infective inflammation imaging using  $^{99m}\text{Tc}$  eluted from  $^{99}\text{Mo}/^{99m}\text{Tc}$  generator based on zirconium molybdate. *Appl Radiat Isot* 68:1959–1963
31. Abdou ES, Nagy KSA, Elsabee MZ (2008) Extraction and characterization of chitin and chitosan from local sources. *Bioresour Technol* 99:1359–1367
32. Chang BKL, Tsai G, Lee J, Fu WR (1997) Heterogeneous N-deacetylation of chitin in alkaline solution. *Carbohydr Res* 303:327–332
33. Broussignac P (1968) Chitosan, a natural polymer not well known by the industry. *Chim Ind Gene Chim* 99:1241–1247
34. Gano L, Patricio L, Castanheira I (1989) *J Radioanal Nucl Chem* 132:171–178
35. Kim EM, Jeong HJ, Park IK, Cho CS, Kim CG, Bom HS (2005) Hepatocyte-targeted nuclear imaging using  $^{99m}\text{Tc}$ -galactosylated chitosan: conjugation, targeting, and biodistribution. *J Nucl Med* 46:141–145
36. Kasaai R, Arul J, Charlet G (2000) Intrinsic viscosity–molecular weight relationship for chitosan. *J Polym Sci B* 88:2591–2598
37. Domard A (1987) Determination of N-acetyl content in chitosan samples by c.d. measurements. *Int J Biol Macromol* 9:333–336
38. Chandumpai A, Singhpibulporn N, Faroongsarng D, Somprasit P (2004) Preparation and physico-chemical characterization of chitin and chitosan from the pens of the squid species, *Loligo lessoniana* and *Loligo formosana*. *Carbohydr Polym* 58:467–474
39. Banerjee T, Singh AK, Sharma RK, Maitra AN (2005) Labeling efficiency and biodistribution of Technetium-99m labeled nanoparticles: interference by colloidal tin oxide particles. *Int J Pharm* 289:189–195
40. Onishi H, Machida Y (1999) Biodegradation and distribution of water soluble chitosan in mice. *Biomaterials* 20:175–182
41. Saha GB (1998) Fundamentals of nuclear pharmacy, 4th edn. Springer-Verlag, New York
42. Park IK, Yang J, Jeong HJ, Bom HS, Harada I, Akaike T, Kim SI, Cho CS (2003) Galactosylated chitosan as a synthetic extracellular matrix for hepatocytes attachment. *Biomaterials* 24:2331–2337